

## **Numerical Simulation of the Carbon Cycle Over The Tibetan Plateau, China**

Authors: Fan, Guangzhou, Zhang, Tingjun, Ji, Jinjun, Li, Kerang, and Liu, Jiyuan

Source: Arctic, Antarctic, and Alpine Research, 39(4) : 723-731

Published By: Institute of Arctic and Alpine Research (INSTAAR), University of Colorado

URL: [https://doi.org/10.1657/1523-0430\(07-502\)\[FAN\]2.0.CO;2](https://doi.org/10.1657/1523-0430(07-502)[FAN]2.0.CO;2)

---

BioOne Complete ([complete.BioOne.org](https://complete.BioOne.org)) is a full-text database of 200 subscribed and open-access titles in the biological, ecological, and environmental sciences published by nonprofit societies, associations, museums, institutions, and presses.

Your use of this PDF, the BioOne Complete website, and all posted and associated content indicates your acceptance of BioOne's Terms of Use, available at [www.bioone.org/terms-of-use](https://www.bioone.org/terms-of-use).

Usage of BioOne Complete content is strictly limited to personal, educational, and non - commercial use. Commercial inquiries or rights and permissions requests should be directed to the individual publisher as copyright holder.

---

BioOne sees sustainable scholarly publishing as an inherently collaborative enterprise connecting authors, nonprofit publishers, academic institutions, research libraries, and research funders in the common goal of maximizing access to critical research.

# Numerical Simulation of the Carbon Cycle over the Tibetan Plateau, China

Guangzhou Fan\*†‡#

Tingjun Zhang†§

Jinjun Ji†

Kerang Li† and

Jiyuan Liu†

\*Chengdu University of Information and Technology, Chengdu 610041, China

†Institute of Geographical Science and Natural Resource Research, Chinese Academy of Sciences, Beijing 100101, China

‡National Snow and Ice Data Center, Cooperative Institute for Research in Environmental Sciences, University of Colorado at Boulder, Boulder, Colorado 80304-0449, U.S.A.

§Chinese Academy of Meteorological Sciences, China Meteorology Administrations, Beijing 800081, China

#Corresponding author: fanggz@cuit.edu.cn

## Abstract

Significant interaction occurs between ecosystem physiological processes and climate. Studying this interaction is beneficial for understanding dynamics of climate change as well as forecasting future climate change. On the Qinghai-Xizang Plateau, the highest plateau in the world, interaction between ecosystem physiological processes and climate affect mid-levels of the atmosphere, so the study of this interaction has a special significance. We use two models, a carbon cycle model (CCM3) and a land surface model (LSM), to simulate ecosystem carbon cycle characteristics over the Tibetan Plateau and its influence on climate. The CO<sub>2</sub> flux varies seasonally with ecosystem physiology processes on the Plateau: fluxes are highest in summer and lowest in winter. The seasonal variation of vegetation net CO<sub>2</sub> flux shows that vegetation is an atmospheric carbon sink during most of the year, except in winter. This means that vegetation could weaken the greenhouse effect, which is important in terms of global warming. The land ecosystem is a weak carbon source from October to April, and it is a carbon sink from May to September (especially between June and August). The Tibetan Plateau CO<sub>2</sub> fluxes vary spatially. The fluxes are highest over the southwest and southeast boundary areas and the northeast region of the Plateau in summer, and are lowest in the middle and northwest regions in winter. The interaction of CO<sub>2</sub> flux and temperature shows that higher temperatures increase vegetation photosynthesis and all respiration. The abrupt increase in land ecosystem physiological processes with increasing temperature indicates that any warming due to increased atmospheric CO<sub>2</sub> caused by human activity will be weakened by the land ecosystem over the Tibetan Plateau.

## Introduction

Vegetation affects the Earth's hydrologic cycle, atmospheric circulation, the thermal characteristics of the Earth's surface, and heat exchange between the surface and the atmosphere. Vegetation interacts with rain and groundwater, affects surface winds and surface albedo, and absorbs and releases atmospheric gases. These interactions affect local, regional, and even global climate.

Vegetation is also significantly affected by climate change. Most historical studies of the interaction of the ecosystem and climate focus on the physical processes that plants are part of (Charney, 1975; Xue et al., 1990; Carlos et al., 1991; Fan et al., 1998; Claussen, et al., 1999). In one study of biogeophysical feedback, Fan et al. (1998) found that if northwestern China were deforested, the annual mean surface temperature would rise and the annual mean sea-level pressure would decrease in eastern and southern Asia. Precipitation would increase in China and the Indochina peninsula, and would decrease in the Indian peninsula. Ground surface heat sources in northwestern China would be clearly strengthened after the deforestation, which would weaken the winter monsoon and strengthen the summer monsoon in eastern and southern Asia. Fan et al. (1998) indicate that vegetation in temperate, arid, semiarid, and tropical rain forest areas affects physical processes differently.

Recently, the interaction between ecosystem physiological processes and climate change has been studied in more depth. For example, vegetation clearly plays an important role in the "greenhouse effect" of increased concentrations of atmospheric CO<sub>2</sub> and this discovery is significant for understanding climate

change (Kabat et al., 1998). By measuring and analyzing changes in the concentration of atmospheric oxygen and the <sup>13</sup>C/<sup>12</sup>C ratio, we have gained a new understanding of current global carbon circulation. Studies have found that mid-latitude ecosystems are important carbon sinks, which can absorb about 2 Gt a<sup>-1</sup> of human-generated CO<sub>2</sub> (Zhang and Sun, 1999). Bonan (1991) used an ecosystem model to study the CO<sub>2</sub> fluxes of 23 forests in Alaska and found that only one forest is a source of CO<sub>2</sub>; the other 22 were all CO<sub>2</sub> sinks. Mora et al. (1996) discovered that during the last half of the Paleozoic, atmospheric CO<sub>2</sub> concentration decreased about 10%, due to an increase in vegetation and the start of the Carboniferous glacier age, caused by climate change. Sellers et al. (1996) simulated the physiological response of vegetation when exposed to an increase in atmospheric CO<sub>2</sub> and found that the CO<sub>2</sub> increase could result in continental warming in addition to the conventional "greenhouse effect," but this relationship was found to be inverse during the growing season. Shi and Guo (1997) indicated that the Earth's ecosystem has a dual action in the global carbon cycle. A halt of human activity would make the Earth a source of atmospheric CO<sub>2</sub>, but the response to the increased CO<sub>2</sub> would be to initiate changes that would create a CO<sub>2</sub> sink. Oechel et al. (2000) showed that the Alaskan tundra reverted to being a carbon sink during the last decade of the 20th century, with decreased carbon release. But during the 1980s, the tundra was a source of carbon. Cox et al. (2000) hypothesized that the Earth's land biosphere will be a carbon sink until 2050, and then become a carbon source. Hu et al. (2001) investigated the effects of elevated CO<sub>2</sub> on grasslands and found that the carbon reserves of the soil increased about 11% after increased CO<sub>2</sub>,

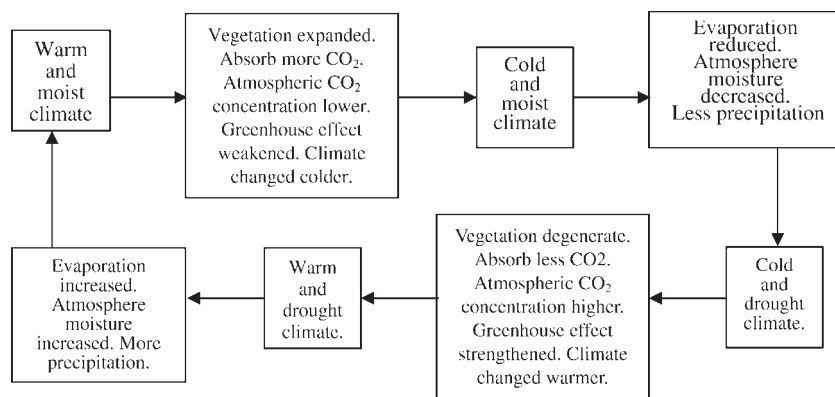


**FIGURE 1.** A simple conceptual model of the interaction between vegetation physiology and climate (Fan and Cheng, 2002).

despite no clear increase in the net primary production. The increased CO<sub>2</sub> concentrations reduced the microbial nitrogen in the soil, resulting in a net accumulation of carbon. Additionally, Schlesinger and Lichter (2001) and Oren et al. (2001) showed that soil and fallen leaves in North Carolina under the trees contain only small amounts of carbon, and this nutrient shortage affects the carbon reserving ability of the trees for the long-term.

These studies have shown that vegetation can effect regional or (and) global climate. Climate change can also clearly affect the distribution of vegetation and the ability of vegetation to absorb atmospheric CO<sub>2</sub>. Christensen et al. (1999) examined the carbon cycle and CH<sub>4</sub> exchange in a vertical section of tundra in Eurasia, and found that the long-term carbon accumulation ratio (net absorption of atmospheric CO<sub>2</sub>) is influenced by climate parameters (such as the average temperature in July, and annual precipitation). With higher temperatures and/or greater precipitation, the carbon absorbing velocity was increased.

Fan and Cheng (2002) used a land surface model to simulate the interaction between the physiological processes of Tibetan Plateau vegetation and climate during the summer monsoon. They showed that the Plateau vegetation physiological processes are clearly affected by climate and the CO<sub>2</sub> concentration of the atmosphere. Higher temperatures, greater soil moisture, and higher CO<sub>2</sub> concentrations benefit photosynthesis and respiration. Vegetation absorbs CO<sub>2</sub>, weakening any warming due to the CO<sub>2</sub> “greenhouse effect.” Fan and Cheng (2002) then created a simple conceptual model of the interaction between vegetation physiological processes and climate (Fig. 1). Vegetation increases when climate is warm and moist. Increased vegetation absorbs more CO<sub>2</sub> reducing the CO<sub>2</sub> concentration and weakening the greenhouse effect. This cools the climate, decreasing evaporation. This can then decrease atmospheric moisture and precipitation, which can create a cold, dry climate. The cold and the drought conditions decrease vegetation, which decreases CO<sub>2</sub> absorption. The CO<sub>2</sub> concentrations then cause climate warming. Evaporation is increased, along with atmospheric moisture precipitation. The climate then changes to warm and rainy climate, and the cycle is complete. This feedback can be called “biogeochemical feedback” as the “biogeophysical feedback” advanced by Charney (1975).

There have been various studies on the interaction between land ecosystems and climate change, but each of these studies was in a different area, at different times, and used different methods. The Qinghai-Xizang Plateau (the highest plateau in the world) is located in this mid-latitude area. Its ecosystem influences climate change and directly affects the upper atmosphere. The modeling study of Fan and Cheng (2002) used a one-grid land surface model, and only modeled the summer monsoon. That study only

simulated the interaction between the vegetation physiology processes and climate, and did not consider the influence of microorganism respiration. Therefore, it did not present the entire interaction between the ecosystem and climate over the Plateau. Researchers have also not studied the spatial and temporal distribution and variation of carbon cycle over the Tibetan Plateau. Our study used a land surface model (LSM mainly used to test the simulation ability of CCM3—Community Climate Model Version 3) and CCM3 to simulate the spatial and temporal distribution and variation of carbon circulation over the Tibetan Plateau and its possible influence on climate.

## Models and Experiments

### LSM MODEL AND EXPERIMENT DESIGN

#### LSM Introduction

The land surface model (LSM1.0) was developed by Bonan (1996). It is a one-dimensional model that includes dynamic ecosystem processes such as biophysical processes, hydrological processes, and biochemical processes. It can be used to model the exchanges of energy, momentum, moisture, and CO<sub>2</sub> between the land and the atmosphere. The CO<sub>2</sub> exchange in the model includes vegetation photosynthesis, vegetation respiration, and microorganism respiration. The CO<sub>2</sub> absorbing rate of photosynthesis is related as ( $\mu\text{mol s}^{-1} \text{m}^{-2}$ )

$$A = \frac{C_s - C_i}{1.65r_s p_{\text{atm}}}$$

where  $C_s$  is the CO<sub>2</sub> concentration at the leaf surface (Pa),  $C_i$  is the internal leaf CO<sub>2</sub> concentration (Pa),  $r_s$  is leaf stomatal resistance ( $\text{s m}^2 \mu\text{mol}^{-1}$ ), and  $p_{\text{atm}}$  is atmospheric pressure (Pa).

CO<sub>2</sub> loss during plant respiration is broken into maintenance respiration and growth respiration. The maintenance respiration  $R_m$  ( $\mu\text{mol s}^{-1} \text{m}^{-2}$ ) is

$$R_m = [LR_{f25}f(N)\beta_t + V_b^s R_{s25} + V_b^r R_{r25}] a_{rm}^{\frac{T_v - 25}{10}}$$

where  $L$  is the leaf area index ( $\text{m}^2 \text{m}^{-2}$ ),  $R_{f25}$  is the foliage respiration at 25°C ( $\mu\text{mol s}^{-1} \text{m}^{-2}$ ),  $V_b^s$  is the stem biomass ( $\text{kg m}^{-2}$ ),  $R_{s25}$  is the stem respiration at 25°C ( $\mu\text{mol s}^{-1} \text{kg}^{-1}$ ),  $V_b^r$  is the root biomass ( $\text{kg m}^{-2}$ ),  $R_{r25}$  is the root respiration at 25°C ( $\mu\text{mol s}^{-1} \text{kg}^{-1}$ ),  $T_v$  is the vegetation temperature (°C), and  $a_{rm}$  is a temperature sensitivity parameter.  $f(N)$  is the foliage nitrogen factor, and  $\beta_t$  is the soil water factor. The growth respiration  $R_g$  ( $\mu\text{mol s}^{-1} \text{m}^{-2}$ ) is

$$R_g = 0.25(A_{\text{sun}}L_{\text{sun}} + A_{\text{sha}}L_{\text{sha}}).$$

where  $A_{sun}$  and  $A_{sha}$  are the sunlit and shaded leaf photosynthesis, respectively, and  $L_{sun}$  and  $L_{sha}$  are the sunlit and shaded leaf area indices.

Microbial respiration  $R_s$  ( $\mu\text{mol s}^{-1} \text{m}^{-2}$ ) is

$$R_s = \frac{\bar{\theta}}{a_1 + \bar{\theta} a_2 + \bar{\theta}} a_2 a_3 S_c a_4^{\frac{T_s - 10}{10}}$$

where  $\bar{\theta}$  is the volumetric soil water content to a depth of 1 m,  $a_1$  is one-half field capacity,  $a_2$  is one-half saturation,  $S_c$  is soil carbon ( $\text{kg m}^{-2}$ ),  $a_3$  is the respiration rate ( $\mu\text{mol CO}_2 \text{kgC}^{-1} \text{s}^{-1}$ ) at  $10^\circ\text{C}$ ,  $a_4$  is a temperature sensitivity parameter, and  $T_s$  is the temperature ( $^\circ\text{C}$ ) of the first soil layer.

#### LSM Input Data

The atmospheric boundary conditions required by the LSM include

- (1) atmospheric reference height ( $z_{atm}$ )
- (2) pressure at  $z_{atm}$
- (3) temperature at  $z_{atm}$
- (4) zonal wind at  $z_{atm}$
- (5) meridional wind at  $z_{atm}$
- (6) specific humidity at wind at  $z_{atm}$
- (7) surface pressure
- (8) large-scale precipitation
- (9) convective precipitation
- (10) partial pressure  $\text{CO}_2$  at  $z_{atm}$  ( $355 \times 10^{-6} \text{mol mol}^{-1}$ )
- (11) partial pressure  $\text{O}_2$  at  $z_{atm}$  ( $0.209 \text{mol mol}^{-1}$ )
- (12) incident direct beam solar radiation ( $<0.7 \mu\text{m}$ )
- (13) incident direct beam solar radiation ( $\geq 0.7 \mu\text{m}$ )
- (14) incident diffuse solar radiation ( $<0.7 \mu\text{m}$ )
- (15) incident diffuse solar radiation ( $\geq 0.7 \mu\text{m}$ )
- (16) incident longwave radiation.

The physical variables from (1) to (9) and (16) are given by the GAME (GEWEX Asia Monsoon Experiment)/Tibet experiment, which was a 3-mo enhanced observation from 16 June to 16 September 1998 over the Ando area ( $32^\circ 14' 30''\text{N}$ ,  $91^\circ 37' 30''\text{E}$ ). Quality analysis and error information are given by Ishikawa et al. (1999).

The four radiation variables are calculated by exponential formula:

$$\text{Incident direct beam solar radiation } F_{s,b} = \lambda_d (1 - \lambda_b) F_{sw}$$

$$\text{Incident diffuse solar radiation } F_{s,d} = \lambda_d \lambda_b F_{sw}$$

$$\text{Incident direct beam solar radiation } F_{n,b} = (1 - \lambda_d)(1 - \lambda_b) F_{sw}$$

$$\text{Incident diffuse solar radiation } F_{n,d} = (1 - \lambda_d) \lambda_b F_{sw}$$

where

$$\lambda_b = \beta + (1 - \beta) C_t$$

$$\beta = \frac{0.0604}{\cos\theta - 0.0223} + 0.0683,$$

$$\lambda_d = \frac{580 - 464 C_t}{(580 - 499 C_t) + (580 - 464 C_t)},$$

$F_{sw}$  is the total shortwave radiation of the land surface,  $\cos\theta$  is the solar zenith angle, and  $C_t$  is cloud cover.

The land surface parameters of LSM1.0 include the longitude and latitude of the center of the grid cell, the surface type, the soil color type, etc. The longitude and latitude are used to calculate the solar zenith angle. The surface type is used to confirm the vegetation type and its fractional cover. The model includes 29 land surface types and 14 vegetation types. Every land surface type

includes three vegetation types and the fractional cover. The soil color is used to confirm the drought and wet soil albedo. These parameters are presented by Bonan (1996).

#### LSM Experiment Design

The LSM experiment uses the GAME/Tibet observed data and calculated radiation data in addition to measured land surface data. The experiment ran from 0000 h on 16 June to 2400 h on 16 September 1998, with a time interval of 5 min.

Because the temporal coverage of directly observed carbon cycle data is very short, the CCM3 simulated carbon cycle fluxes over the Tibetan Plateau cannot be tested with observed data. But the LSM experiment driven data are mainly the observed data discussed as in LSM Input Data (above). The modeling results might be quite reasonable, so the LSM results can be compared to the CCM3 results to test the CCM3 modeling energy.

#### CCM3 INTRODUCTION AND EXPERIMENT DESIGN

CCM3 (Community Climate Model Version 3) was developed by the National Center for Atmospheric Research (NCAR). It has been well tested and is broadly used to simulate global atmospheric circulation, precipitation, and temperature. This study tested CCM3's simulation of the carbon cycle.

The vertical coordinate used in CCM3 is a hybrid sigma-pressure system that includes 18 levels. The horizontal coordinate used triangular truncation 42 waves (T42). The models spatial coverage is about  $2.5^\circ$  longitude by  $2.5^\circ$  latitude. The integral time step is 20 min. The terrain, land surface character, sea temperature, and land-sea distribution data are observed data. The model is coupled one time for every month. The land surface model coupled in CCM3 is LSM. The model is initialized on 15 April 1986 and ends on 28 February 1993 about seven integral years. The first 2 yr of data are released. Only the last 5 yr of data (from 1 March 1988 to 28 February 1993) are used for analysis. The experiment includes five growing seasons.

### Ability of CCM3 to Simulate the Carbon Cycle

#### SIMULATION OF THE GLOBAL CARBON CYCLE

Bonan (1998) used CCM3/LSM1.0 to simulate the carbon cycle for the Tibetan Plateau region. The results showed that the model could simulate  $\text{CO}_2$  fluxes quite well. So in this paper, we will simply test the ability of CCM3 to simulate the carbon cycle.

Figure 2 shows a time/longitude cross-section of mean net  $\text{CO}_2$  flux (the vegetation photosynthesis absorption of  $\text{CO}_2$  minus the vegetation respiration release of  $\text{CO}_2$ ), simulated by CCM3/LSM1.0. Net  $\text{CO}_2$  flux is lowest at about  $60^\circ\text{S}$  and near the North Pole. This is because these areas are mainly composed of ocean. Photosynthesis and respiration are at their highest levels in the summer (from April to September) over the middle latitudes of the Northern Hemisphere ( $40^\circ\text{N}$  to  $65^\circ\text{N}$ ), and the net  $\text{CO}_2$  flux is correspondingly high. Thus, the mid-latitude vegetation ecosystem may be the most important atmospheric carbon sink in the global land ecosystem. It can weaken the global climate warming. Northern Hemisphere mid-latitude  $\text{CO}_2$  flux is negative during the winter (from December to January). The vegetation net  $\text{CO}_2$  flux at the equator area is greater than at other sites, except the northern mid-latitudes.

In the Southern Hemisphere,  $\text{CO}_2$  flux (including vegetation photosynthesis, vegetation respiration, vegetation net flux, micro-

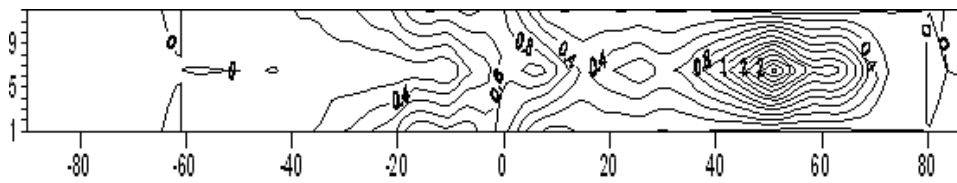


**FIGURE 2.** Time/longitude cross-section of monthly grids mean net CO<sub>2</sub> flux, simulated by CCM3. The abscissa is latitude, the ordinate is month. The units are  $\mu\text{mol s}^{-1} \text{m}^{-2}$ .

organism respiration, and land ecosystem net flux) is highest in January. The land ecosystem net flux over most of the Southern Hemisphere is positive, with the largest fluxes over the tropical rain forest areas. The fluxes of the Northern Hemisphere are lower in January, especially in the area to the north of 30°N, where the land ecosystem net flux is negative during January. This means that the land ecosystem is a carbon sink. As the year progresses, the areas of highest flux gradually move north, reaching their northernmost position in July. At the same time, the fluxes in the Southern Hemisphere diminish, becoming negative over the entire Southern Hemisphere except for the area near the equator. In July, most areas of the Northern Hemisphere CO<sub>2</sub> have positive fluxes. After July, the areas of highest CO<sub>2</sub> flux gradually move south. These flux distribution characteristics generally agree with previous studies, confirming that CCM3 simulation of the land ecosystem carbon cycle is credible.

The mean annual vegetation photosynthesis over the global grids (ocean and land grids) is about  $0.55 \mu\text{mol s}^{-1} \text{m}^{-2}$  and the mean annual respiration is about  $0.32 \mu\text{mol s}^{-1} \text{m}^{-2}$ . Thus the global mean absorbing net CO<sub>2</sub> flux for surface plants is about  $0.23 \mu\text{mol s}^{-1} \text{m}^{-2}$  every year. This shows that vegetation can absorb about 10 Gt of atmospheric CO<sub>2</sub> every year, excluding microorganism respiration. The simulated microorganism respiration is about  $0.17 \mu\text{mol s}^{-1} \text{m}^{-2}$ . Therefore, taking into consideration the microorganism respiration, the land ecosystem can absorb about 2.6 Gt CO<sub>2</sub> every year. This is approximately 30% higher than the CO<sub>2</sub> amounts found by Zhang and Sun (1999), but they only measured carbon absorption in the middle latitudes of the Northern Hemisphere. The CCM3 simulation results presented here are consistent with the other study results.

#### COMPARISON OF TIBETAN PLATEAU CARBON CYCLE FLUXES OF LSM AND CCM3

As previously asserted, the reliability of using CCM3 to simulate the carbon cycle over the Tibetan Plateau cannot be tested because of the lack of observational data. Therefore, we used LSM and the GAME/Tibet data and compared them to the CCM3 results to test the reliability of CCM3. The results of the LSM experiment may be more reliable because it is driven by the observed data. Because the simulation period of LSM is from 16 June to 16 September 1998, and the simulated area is one point (Ando area), only the July and August results from the area

nearest to Ando can be compared. The Ando land surface type is cool grassland. It means that the vegetation type include cool grass (plant cover is about 60%), warm grass (plant cover is about 20%) and bare (plant cover is about 20%).

Table 1 shows the comparison of the LSM and CCM3 simulations of CO<sub>2</sub> fluxes over the Ando area in July and August. The simulated fluxes from each model show little deviation from one another. The greatest variation is in vegetation respiration in August, with an error of about 33.3%. We conclude that the CCM3 simulated CO<sub>2</sub> fluxes over the Tibetan Plateau are credible, and that CCM3 could be used to simulate the land ecosystem physiological carbon cycle over the Tibetan Plateau and its influence on climate.

### Characteristics of the Land Ecosystem Carbon Cycle over the Tibetan Plateau

#### SEASONAL CHARACTERISTICS OF THE CARBON CYCLE

This study only analyzed the seasonal variation of CCM3-simulated land ecosystem carbon fluxes over the Tibetan Plateau (those areas higher than 3000 m).

Vegetation photosynthesis, vegetation respiration, and vegetation net CO<sub>2</sub> flux are highest in summer (from June to August), with maximum values of  $2.72 \mu\text{mol s}^{-1} \text{m}^{-2}$ ,  $1.17 \mu\text{mol s}^{-1} \text{m}^{-2}$ , and  $1.57 \mu\text{mol s}^{-1} \text{m}^{-2}$ , respectively (Fig. 3). These maximums are the 75.6%, 67.8%, and 83.7% of their respective annual means. In winter (December to February), vegetation photosynthesis and vegetation respiration are only  $0.03 \mu\text{mol s}^{-1} \text{m}^{-2}$  and  $0.05 \mu\text{mol s}^{-1} \text{m}^{-2}$ , respectively, and vegetation net CO<sub>2</sub> flux becomes negative (about  $-0.02 \mu\text{mol s}^{-1} \text{m}^{-2}$ ). Therefore, the vegetation system over the Tibetan Plateau is an atmospheric carbon source in winter.

During the spring (March to May), vegetation photosynthesis, vegetation respiration, and vegetation net CO<sub>2</sub> flux are  $0.43 \mu\text{mol s}^{-1} \text{m}^{-2}$ ,  $0.27 \mu\text{mol s}^{-1} \text{m}^{-2}$ , and  $0.17 \mu\text{mol s}^{-1} \text{m}^{-2}$ , respectively. In autumn (September to November), these parameters are  $0.42 \mu\text{mol s}^{-1} \text{m}^{-2}$ ,  $0.26 \mu\text{mol s}^{-1} \text{m}^{-2}$ , and  $0.16 \mu\text{mol s}^{-1} \text{m}^{-2}$ . The spring values are 12%, 15.6%, and 9% of their annual mean values, and the autumn values are 11.7%, 15%, and 8% of the annual means. The carbon sink effect from vegetation is greatest in summer over the Tibetan Plateau, with a milder effect in spring and autumn.

**TABLE 1**  
LSM and CCM3 simulations of CO<sub>2</sub> fluxes near Ando (units are  $\mu\text{mol s}^{-1} \text{m}^{-2}$ ).

		Photosynthesis	Vegetation respiration	Vegetation net flux	Microorganism respiration	Land ecosystem net flux
LSM	July	2.8	1.0	1.8	0.2	1.6
CCM3	July	2.9	1.2	1.7	0.1	1.6
LSM	August	1.8	0.6	1.2	0.3	0.9
CCM3	August	1.9	0.8	1.1	0.1	1.0

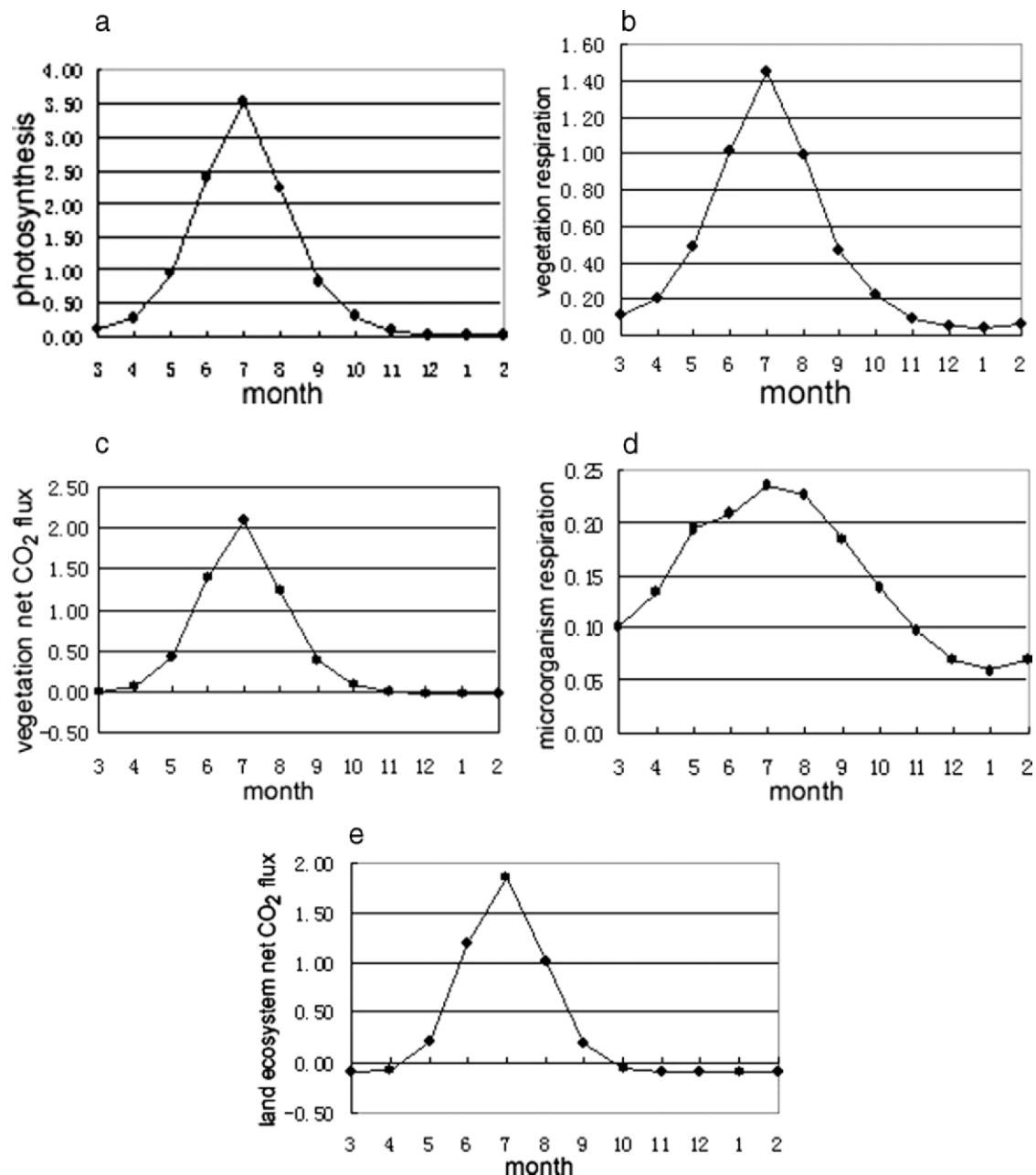


FIGURE 3. CCM3-simulated seasonal variation of CO<sub>2</sub> fluxes over the Tibetan Plateau. (a) Vegetation photosynthesis. (b) Vegetation respiration. (c) Vegetation net CO<sub>2</sub> flux. (d) Microorganism respiration. (e) Land ecosystem net CO<sub>2</sub> flux. All plots have units of in  $\mu\text{mol s}^{-1} \text{m}^{-2}$ . Positive photosynthesis values indicate a flux from the atmosphere to vegetation. Positive respiration values indicate a flux to the atmosphere from vegetation. Positive net fluxes indicate a flux to the atmosphere.

The microorganism respiration over the Tibetan Plateau is highest in summer and lowest in winter, but it has less seasonal variation than vegetation photosynthesis and respiration (Fig. 3). The CCM3-simulated microorganism respiration was  $0.23 \mu\text{mol s}^{-1} \text{m}^{-2}$  (39.5% of the annual mean) in summer,  $0.07 \mu\text{mol s}^{-1} \text{m}^{-2}$  (11.6% of the annual mean) in winter,  $0.15 \mu\text{mol s}^{-1} \text{m}^{-2}$  (25.6% of the annual mean) in spring, and  $0.14 \mu\text{mol s}^{-1} \text{m}^{-2}$  (24.4% of the annual mean) in autumn.

The land ecosystem net flux is negative from October to April, during which the land ecosystem releases CO<sub>2</sub> to the atmosphere as a weak carbon source (Fig. 3). From May to September, the land ecosystem becomes an atmospheric carbon sink, with the greatest carbon sink effect occurring between June and August ( $1.35 \mu\text{mol s}^{-1} \text{m}^{-2}$ ).

#### TEMPORAL/SPATIAL CHARACTERISTICS OF THE CARBON CYCLE

Using the 5-yr averaged monthly mean data, we study the temporal/spatial characteristics of the carbon cycle for the Tibetan Plateau (Fig. 4).

Vegetation photosynthesis displays notable spatial variation over the Tibetan Plateau (Fig. 4a) as well as temporal variation. Vegetation photosynthesis is about  $0 \mu\text{mol s}^{-1} \text{m}^{-2}$  in January over most areas of the Tibetan Plateau (not shown), but is slightly above zero over the southeast boundary area. After January, photosynthesis over the Plateau gradually increases, especially in the east and the northeast, remaining at zero only in the west and northwest before April. Thereafter, photosynthesis increases over the entire Plateau until July. Photosynthesis along the southwest

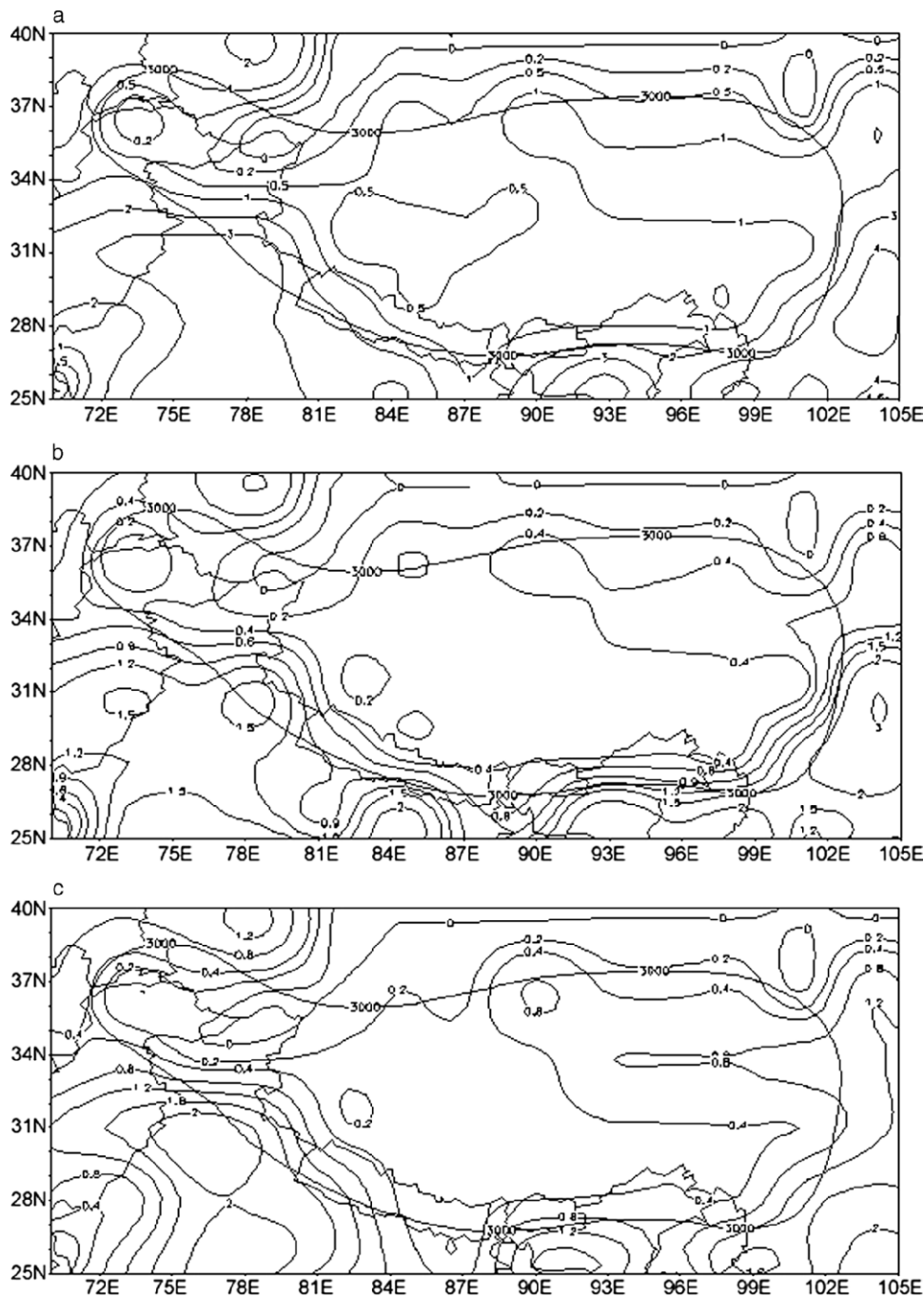


**FIGURE 4.** Spatial distribution of annual mean CO<sub>2</sub> fluxes over the Tibetan Plateau. (a) Vegetation photosynthesis. (b) Vegetation respiration. (c) Vegetation net CO<sub>2</sub> flux. (d) Microorganism respiration. (e) Land ecosystem net CO<sub>2</sub> flux. All plots show fluxes contoured in units of  $\mu\text{mol s}^{-1} \text{m}^{-2}$ .

boundary, the east boundary and in northeast areas are highest, with values of  $10 \mu\text{mol s}^{-1} \text{m}^{-2}$ ,  $6 \mu\text{mol s}^{-1} \text{m}^{-2}$ , and  $5 \mu\text{mol s}^{-1} \text{m}^{-2}$ , respectively. After July, photosynthesis gradually weakens, with reduced center values and ranges, until it again is zero in November in most areas. Spatial variation of photosynthesis is greatest on the south boundary of the Plateau due to the variability in vegetation over the terrain.

The temporal/spatial variation of vegetation respiration over the Tibetan Plateau is similar to the variation of photosynthesis (Fig. 4b). In January, vegetation respiration is greatest in the southern and eastern boundary areas, with low respiration in all other areas (not shown). Vegetation respiration gradually increases between January and July, with mean values of  $4 \mu\text{mol s}^{-1} \text{m}^{-2}$ ,

$3 \mu\text{mol s}^{-1} \text{m}^{-2}$ , and  $2 \mu\text{mol s}^{-1} \text{m}^{-2}$  at the southwest boundary, southeast boundary, and in the northeast, respectively. The difference between respiration and photosynthesis is that respiration increases earlier than photosynthesis in the spring.

The vegetation net CO<sub>2</sub> flux (Fig. 4c) is equal to vegetation photosynthesis minus vegetation respiration. During January and February, the vegetation net flux is negative over most of the Tibetan Plateau, except its southeast boundary (more photosynthesis than respiration) (not shown). Thus, the vegetation system is a carbon source. From February to March, the vegetation net CO<sub>2</sub> flux becomes positive over the southwest, south, southeast, and east boundaries, and over a part of the northeast Plateau. These areas then become a carbon sink. Net CO<sub>2</sub> flux continues to

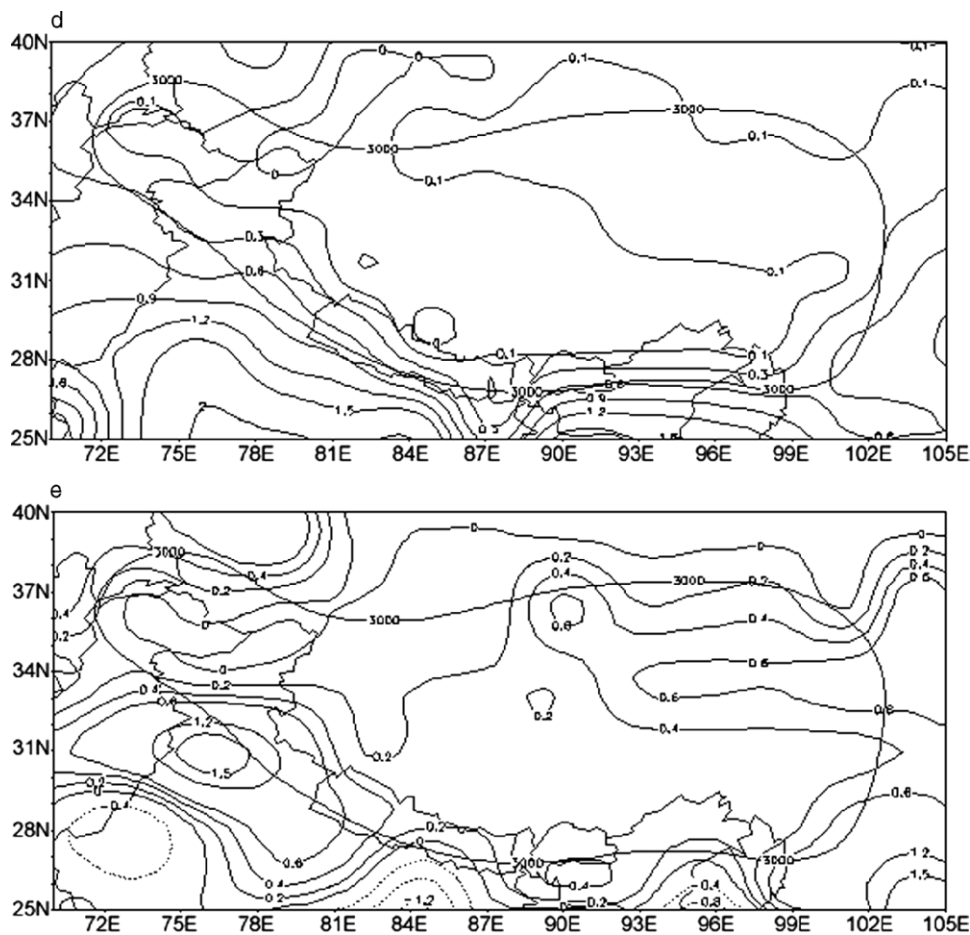


FIGURE 4. Continued.

increase and spread until July, when the net flux is positive across most of the Plateau except in a small northwest area. After July, the vegetation net CO<sub>2</sub> flux decreases and contracts from the western and central areas, and the vegetation becomes a carbon source until November, except in the southwest boundary area of the Plateau.

The soil microorganism respiration varies spatially across the Tibetan Plateau (Fig. 4d), as well as temporally (not shown). Microorganism respiration gradually increases from January to July and then gradually decreases, similar to the temporal variation of vegetation respiration. Spatially, the distribution of annual mean microorganism respiration is similar to that of the vegetation CO<sub>2</sub> fluxes (Fig. 4d). Microorganism respiration is highest in the southwest, along the southern boundary, and in the northeast of the Plateau.

Figure 4e shows that most areas of the Tibetan Plateau are carbon sinks, except for a small area in the northwest Plateau. During January and February, the land ecosystem net CO<sub>2</sub> flux (equal to the vegetation net CO<sub>2</sub> flux minus microorganism respiration) is negative across the Tibetan Plateau (photosynthesis is less than respiration). Thus, the land ecosystem is a carbon source to the atmosphere. Between March and May, the net CO<sub>2</sub> flux becomes positive in the southwest, south, and eastern boundary areas are carbon sinks. Net CO<sub>2</sub> flux is highest in July, across the Plateau. After September, CO<sub>2</sub> flux decreases, and the carbon sink effect of the land ecosystem gradually weakens. By October, most areas of the Plateau become a carbon source, except the southwest, south, and eastern boundary areas, and a small

area in the northeast. Net CO<sub>2</sub> fluxes in November and December are similar to those of January.

### CO<sub>2</sub> Flux Changes with Temperature

Some preliminary simulations with CCM3/LSM0.0 showed that simple physiological and ecological assumptions can result in reasonable simulation of land-atmosphere CO<sub>2</sub> exchange, as compared to observed estimates of annual net primary production and annual microbial respiration (Bonan, 1995). In this paper, we used CCM3/LSM1.0 to study the CO<sub>2</sub>-temperature relationship.

There is a definite intra-annual temporal and spatial distribution of CO<sub>2</sub> fluxes over the Tibetan Plateau, caused by seasonal changes. These seasonal changes are caused by solar radiation and accompanying temperature variations. Analyzing the relationship between temperature change and land ecosystem CO<sub>2</sub> flux will aid in the understanding of the interactions between the ecosystem carbon cycle and climate. Our CCM3 simulation spanned 60 mo (about five growing seasons), giving us 60 monthly mean temperatures over the Tibetan Plateau. Figure 5 shows CO<sub>2</sub> flux variations with temperature.

Vegetation photosynthesis increases with increasing temperature (Fig. 5a). There are three abrupt change periods. At low temperatures, photosynthesis over the Tibetan Plateau is low (about 0 μmol s<sup>-1</sup> m<sup>-2</sup>), but an abrupt change happens when the temperature reaches about 4°C and photosynthesis rises to 0.9 μmol s<sup>-1</sup> m<sup>-2</sup>. The second abrupt change occurs at about 7.3°C when photosynthesis increases to about 2.25 μmol s<sup>-1</sup> m<sup>-2</sup>.

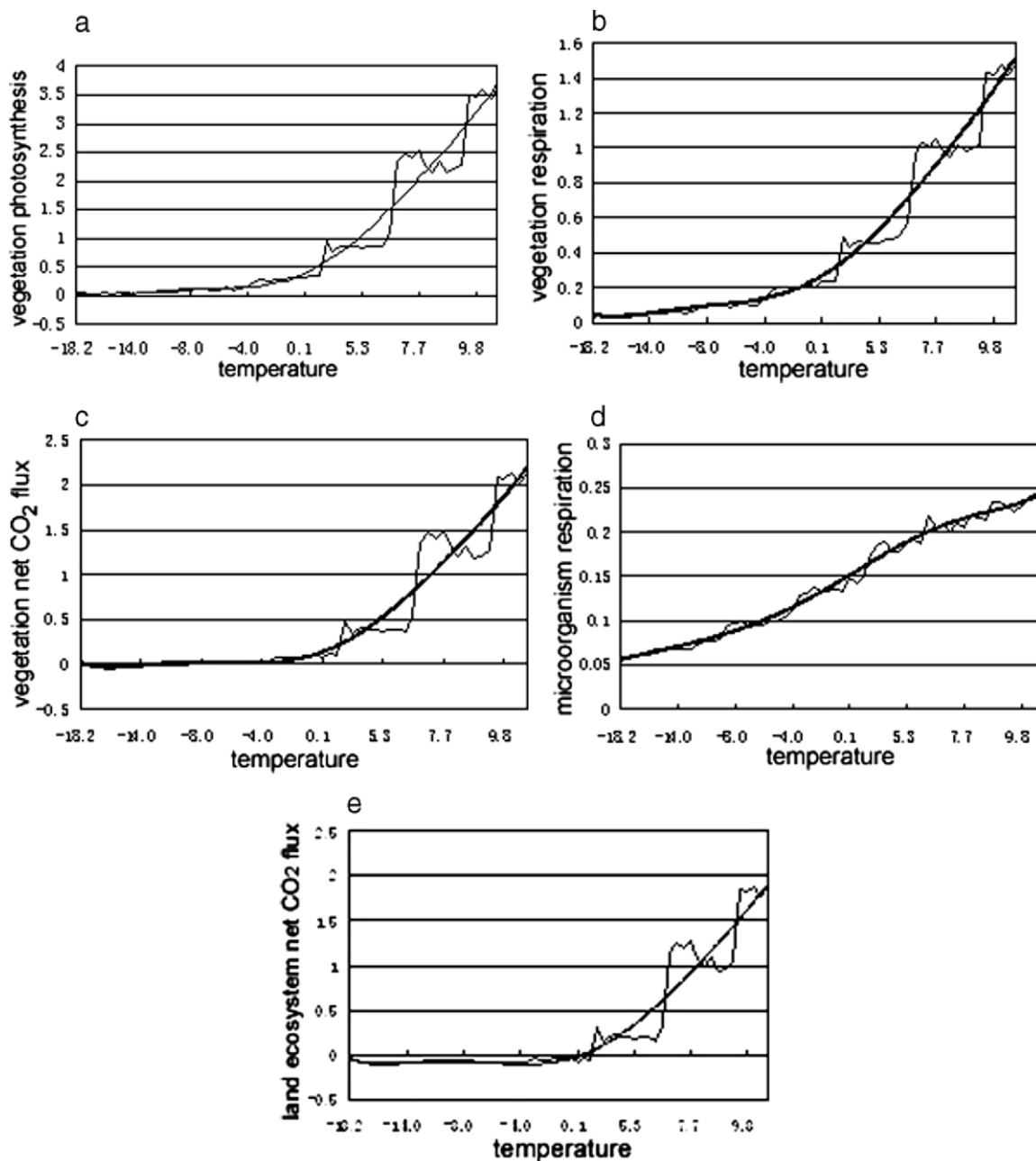


FIGURE 5. Monthly mean CO<sub>2</sub> flux and temperature. (a) Vegetation photosynthesis. (b) Vegetation respiration. (c) Vegetation net CO<sub>2</sub> flux. (d) Microorganism respiration. (e) Land ecosystem net CO<sub>2</sub> flux. All fluxes are in  $\mu\text{mol s}^{-1} \text{m}^{-2}$ , and temperatures are in  $^{\circ}\text{C}$ . Smooth curves show 6th order polynomial fits.

The third change occurs when the temperature reaches about  $9.7^{\circ}\text{C}$  and photosynthesis is  $3.5 \mu\text{mol s}^{-1} \text{m}^{-2}$ .

Vegetation respiration changes with temperature, in a manner similar to that of the photosynthesis change (Fig. 5b). As temperature rises, vegetation respiration increases nonlinearly, with three abrupt changes when the temperature is about  $4^{\circ}\text{C}$ ,  $7.3^{\circ}\text{C}$ , and  $9.7^{\circ}\text{C}$ .

Vegetation net CO<sub>2</sub> flux is less than 0 when the temperature is lower than  $-8^{\circ}\text{C}$  (Fig. 5c), and the vegetation is thus a carbon source. With rising temperatures, the vegetation net CO<sub>2</sub> flux increases nonlinearly, with three abrupt changes occurring when the temperature is  $4^{\circ}\text{C}$ ,  $7.3^{\circ}\text{C}$ , and  $9.7^{\circ}\text{C}$ . Vegetation thus absorbs more atmospheric CO<sub>2</sub> over the Tibetan Plateau with rising temperatures, and the vegetation physiological processes could

weaken the greenhouse effect caused by human activity on the Plateau.

Microorganism respiration increases in a quasi-linear fashion with increasing temperatures (Fig. 5d). Land ecosystem net CO<sub>2</sub> flux is less than 0 when the temperature is lower than  $4^{\circ}\text{C}$  (Fig. 5e), and the land ecosystem is thus a carbon source. With rising temperatures, the vegetation net CO<sub>2</sub> flux increases nonlinearly, with three abrupt changes occurring when the temperature is  $4^{\circ}\text{C}$ ,  $7.3^{\circ}\text{C}$ , and  $9.7^{\circ}\text{C}$ .

Because the land ecosystem net CO<sub>2</sub> flux increases with rising temperature, the ability of the land ecosystem to absorb atmospheric CO<sub>2</sub> over the Tibetan Plateau also increases with temperature, which means that the land ecosystem could weaken the greenhouse effect caused by human activity on the Plateau.

The flux jumps at discrete temperatures may be an important result, but the reasons are not included in the simulation. An improved study on the vegetation physiological process is needed.

## Discussion and Conclusions

This study used CCM3 to simulate the ecosystem carbon cycle over the Tibetan Plateau, and its interaction with the climate. The results show that CO<sub>2</sub> flux varies seasonally with the ecosystem physiology processes on the Plateau. The CO<sub>2</sub> fluxes are highest in summer and lowest in winter. The seasonal variation of vegetation net CO<sub>2</sub> flux shows that vegetation is an atmospheric carbon sink during most of the year, except in winter. This means that the vegetation could weaken the greenhouse effect, which is important in terms of global warming. The land ecosystem net CO<sub>2</sub> flux shows that the land ecosystem is a weak carbon source from October to April, and is a carbon sink from May to September (especially between June and August).

The Tibetan Plateau CO<sub>2</sub> fluxes vary spatially. The fluxes are highest over the southwest and southeast boundary areas and the northeast region of the Plateau in summer, and are lowest in the middle and northwest regions in winter.

The interaction of CO<sub>2</sub> flux and temperature shows that higher temperatures increase vegetation photosynthesis, vegetation respiration, and microorganism respiration. The abrupt increase in the land ecosystem physiological processes with increasing temperature indicates that any greenhouse effect due to increased atmospheric CO<sub>2</sub> caused by human activity will be weakened by the land ecosystem over the Tibetan Plateau. Thus the ecosystem over the Tibetan Plateau has the ability to adjust or moderate the greenhouse effect.

This study was conducted using two simple numerical experiments, and the results were not tested with observed data. This is a shortcoming. In addition, the models used in this study have some restrictions. For example, the ecosystem parameters are set and cannot be changed with climate, and the model's atmospheric CO<sub>2</sub> concentration is also set and cannot be changed with ecosystem physiological processes. These shortcomings, and the short simulation runtime, will be addressed in future studies.

## Acknowledgments

This work was supported by: (1) Program of National Natural Science Foundation (40675037), (2) The Key Program of SiChuan Province Youth Science and Technology Fund (05ZQ026-023), and (3) Opening Project of Chengdu Institute of Plateau Meteorology (IPM).

## References Cited

- Bonan, G. B., 1991: Atmosphere-biosphere exchange of carbon dioxide in boreal forests. *Journal of Geophysical Research*, 96(D4): 7301–7312.
- Bonan, G. B., 1995: Land-atmosphere CO<sub>2</sub> exchange simulated by a land surface process model coupled to an atmospheric general circulation model. *Journal of Geophysical Research*, 100(D2): 2817–2831.
- Bonan, G. B., 1996: A Land Surface Model (LSM version 1.0) for Ecological, Hydrological, and Atmospheric studies: Technical Description and User's Guide, NCAR Tech Note NCAR/TN417+STR, 150 pp.
- Bonan, G. B., 1998: The Land Surface Climatology of the NCAR Land Surface Model Coupled to NCAR Community Climate Model. *Journal of Climate*, 11(6): 1307–1326.
- Carlos, A. N., Sellers, P. J., and Shukla, J., 1991: Amazonian deforestation and regional climate change. *Journal of Climate*, 4(10): 957–988.
- Charney, J. G., 1975: Dynamics of deserts and drought in the Sahel. *Quarterly Journal of the Royal Meteorological Society*, 101: 193–202.
- Christensen, T. R., Jonasson, S., Callaghan, T. V., Havström, M., and Livens, F. R., 1999: Carbon cycling and methane exchange in Eurasian tundra ecosystems. *Ambio*, 28(3): 238–244.
- Claussen, M., Kubatzki, C., Brovkin, V., Ganopolski, A., Hoelzmann, P., and Pachur, H.-J., 1999: Simulation of an abrupt change in Saharan vegetation in the mid-Holocene. *Geophysical Research Letters*, 26(14): 2037–2040. doi:10.1029/1999GL900494.
- Cox, P. M., Betts, R. A., Jones, C. D., Spall, S. A., and Totterdell, I. J., 2000: Acceleration of global warming due to carbon-cycle feedbacks in a coupled climate model. *Nature*, 408: 184–187.
- Fan, G., and Cheng, G., 2002: Interaction between the physiological process of the Tibetan Plateau vegetation and the CO<sub>2</sub> concentration and climate change. *Chinese Journal of Atmospheric Science*, 27(4): 509–518. (In Chinese with English abstract.)
- Fan, G., Lu, S., and Luo, S., 1998: The influence of the NW China afforestation on regional climate in east and south Asia. *Plateau Meteorology*, 17(3): 300–309. (In Chinese with English abstract.)
- Hu, S., Chapin, F. S., Firestone, M. K., Field, C. B., and Chiariello, N. R., 2001: Nitrogen limitation of microbial decomposition in a grassland under elevated CO<sub>2</sub>. *Nature*, 409: 188–191.
- Ishikawa, H., Hayashi, T., Tanaka, K., Tsukamoto, O., Fudeyasu, H., and Tamagawa, I., 1999: Summary of Planetary Boundary Layer Observation in GAME/Tibet, Proceedings of the 1st International Workshop on GAME-Tibet, edited by Numaguti Atusi, Liu Liping and Tian Lide, 69–72.
- Kabat, P., Hutjes, R. W. A., and Gash, J., 1998: Land surface data in climate and weather models; the role of land surface in controlling climate is still underestimated. *Biospheric Aspects of the Hydrologic Cycle (BAHC) News*, No. 6, 8–10.
- Mora, C. I., Driese, S. G., and Colarusso, L. A., 1996: Middle to late Paleozoic atmospheric CO<sub>2</sub> levels from carbonate and organic matter. *Science*, 271: 1105–1107.
- Oechel, W. C., Vourlitis, G. L., Hastings, S. J., Zulueta, R. C., Hinzman, L., and Kane, D., 2000: Acclimation of ecosystem CO<sub>2</sub> exchange in the Alaskan Arctic in response to decadal climate warming. *Nature*, 406: 978–981.
- Oren, R., Ellsworth, D. S., Johnsen, K. H., Phillips, N., Ewers, B. E., Maier, C., Schäfer, K. V. R., McCarthy, H., Hendrey, G., McNulty, S. G., and Katul, G. G., 2001: Soil fertility limits carbon sequestration by forest ecosystems in a CO<sub>2</sub>-enriched atmosphere. *Nature*, 411: 469–472.
- Schlesinger, W. H., and Lichten, J., 2001: Limited carbon storage in soil and litter of experiment forest plots under increased atmospheric CO<sub>2</sub>. *Nature*, 411: 466–469.
- Sellers, P. J., Bounoua, L., Collatz, G. J., Randall, D. A., Dazlich, D. A., Los, S. O., Berry, J. A., Fung, I., Tucker, C. J., Field, C. B., and Jensen, T. G., 1996: Comparison of radiative and physiological effects of doubled atmospheric CO<sub>2</sub> on climate. *Science*, 271(8): 1402–1406.
- Shi, G., and Guo, J., 1997: One-dimensional analysis of global carbon cycle. *Chinese Journal of Atmospheric Science*, 22(4): 413–425. (In Chinese with English abstract.)
- Xue, Y., Liou, K.-N., and Kasahara, A., 1990: Investigation of biogeophysical feedback on the African climate using a two-dimensional model. *Journal of Climate*, 3(3): 337–352.
- Zhang, Z., and Sun, C., 1999: Late decade development of the global change study. *Chinese Science Bulletin*, 44(5): 464–477. (In Chinese with English abstract.)

Ms accepted June 2007